

# Introducing 45 nm technology in Microwind3

Etienne SICARD

Professor

INSA-Dgei, 135 Av de Ranguel

31077 Toulouse – France

[www.microwind.org](http://www.microwind.org)

email: [Etienne.sicard@insa-toulouse.fr](mailto:Etienne.sicard@insa-toulouse.fr)

Syed Mahfuzul Aziz

School of Electrical & Information Engineering

University of South Australia

Mawson Lakes, SA 5095, Australia

[www.unisa.edu.au](http://www.unisa.edu.au)

email: [mahfuz.aziz@unisa.edu.au](mailto:mahfuz.aziz@unisa.edu.au)

This paper describes the improvements related to the CMOS 45 nm technology and the implementation of this technology in Microwind3. The main novelties related to the 45 nm technology such as the high-k gate oxide, metal-gate and very low-K interconnect dielectric is described. The performances of a ring oscillator layout and a 6-transistor RAM memory layout are also analyzed.

## 1. Recent trends in CMOS technology

Firstly, we give an overview of the evolution of important parameters such as the integrated circuit (IC) complexity, gate length, switching delay and supply voltage with a prospective vision down to the 22 nm CMOS technology. The trend of CMOS technology improvement continues to be driven by the need to integrate more functions within a given silicon area. Table 1 gives an overview of the key parameters for technological nodes from 180 nm, introduced in 1999, down to 22 nm, which is supposed to be in production around 2011. Demonstration chips using 45-nm technology have been reported starting in 2004. Mass market manufacturing with this technology is scheduled for late 2007.

Technology node	130 nm	90 nm	65 nm	45 nm	32 nm	22 nm
First production	2001	2003	2005	2007	2009	2011
Effective gate length	70 nm	50 nm	35 nm	25 nm	17 nm	12 nm
Gate material	Poly	Poly	Poly	Metal	Metal	Metal
Gate dielectric	SiO <sub>2</sub>	SiO <sub>2</sub>	SiON	High K	High K	High K
K <sub>gates</sub> /mm <sup>2</sup>	240	480	900	1500	2800	4500
Memory point (μ <sup>2</sup> )	2.4	1.3	0.6	0.3	0.15	0.08

Table 1: Technological evolution and forecast up to 2011

The gate material has long been polysilicon, with silicon dioxide (SiO<sub>2</sub>) as the insulator between the gate and the channel (Fig. 1). The atom is a convenient measuring stick for this insulating material beneath the gate, commonly known as gate oxide. In the 90 nm technology, the gate oxide was consisting of about five atomic layers, equivalent to 1.2 nm in thickness. The thinner the gate oxide, the higher the transistor current and consequently the switching speed. However, thinner gate oxide also means more leakage current. The ultimate limit seems to be 1.0 nm as detailed in [Chau2004]. Starting with the 90nm technology, SiO<sub>2</sub> has been replaced by SiON dielectric, which features a higher permittivity and consequently improves the device performances while keeping the parasitic leakage current within reasonable limits. Starting with the 45-nm technology, leakage reduction has been achieved through the use of various high-K dielectrics such as Hafnium Oxide HfO<sub>2</sub> ( $\epsilon_r=12$ ), Zirconium Oxide ZrO<sub>2</sub> ( $\epsilon_r=20$ ), Tantalum Oxide Ta<sub>2</sub>O<sub>5</sub> ( $\epsilon_r=25$ ) or Titanium Oxide TiO<sub>2</sub> ( $\epsilon_r=40$ ). This provides much higher device performance as if the device was fabricated in a technology using conventional SiO<sub>2</sub> with much reduced “equivalent SiO<sub>2</sub> thickness”.

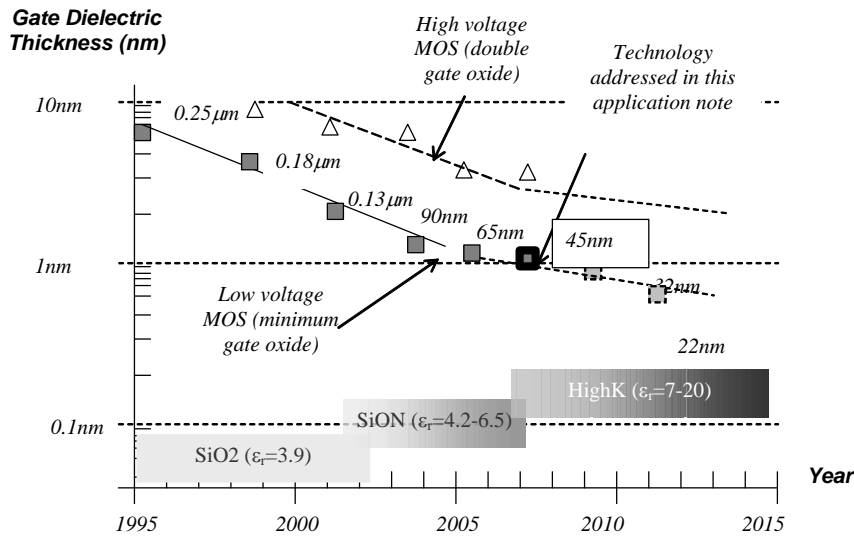


Figure 1 : The technology scale down towards nano-scale devices

The High-K dielectric enabled a thinner “equivalent” oxide thickness while keeping leakage current low. The “equivalent oxide thickness” TOXE is defined by Equ. 1. For the 45-nm technology, the high-K permittivity declared in the rule file is 10 (Parameter “GateK”). The physical oxide thickness is 3.5 nm, and by applying equ. 1, TOXE is 1.4nm. These parameters are in close agreement with those in Song’s review on 45-nm gate stacks [Song2006].

$$TOXE = \left( \frac{\epsilon_{SiO2}}{\epsilon_{high-k}} t_{high-k} \right) \quad (\text{Equ. 1})$$

Where

$\epsilon_{SiO2}$  = dielectric permittivity of SiO2 (3.9, no unit)

$\epsilon_{high-k}$  = High-K dielectric permittivity

$t_{high-k}$  = High-K oxide thickness (m)

In the 45-nm technology node, some IC manufacturers targeting low cost production have kept the polysilicon gate and the SiON oxide, while still achieving important speed and power improvements, thanks to channel length reduction [Fujitsu2005]. However, IC manufacturers oriented towards very high performances have replaced the SiON oxide by Hafnium Oxide to obtain an equivalent oxide thickness TOXE close to 1.0 nm.

At each lithography scaling, the linear dimensions are approximately reduced by a factor of 0.7, and the areas are reduced by factor of 2. Smaller cell sizes lead to higher integration density which has risen to nearly 2 million gates per mm<sup>2</sup> in the 45-nm technology.

The integrated circuit market has been growing steadily since many years, due to ever-increasing demand for electronic devices. The production of integrated circuits for various technologies over the years is illustrated in Fig. 2. It can be seen that a new technology has appeared regularly every two years, with a ramp up close to three years. The production peak is constantly increased, and similar trends should be observed for novel technologies such as 45nm (forecast peak in 2010).

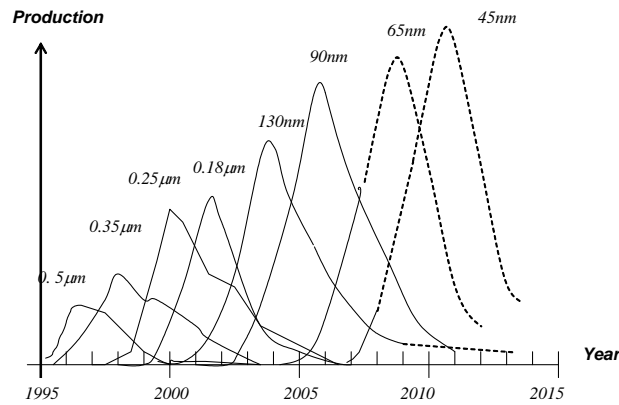


Figure 2 : Technology ramping every two years introducing the 45 nm technology

Prototype 45-nm processes have been introduced by TSMC in 2004 [Tsmc2004] and Fujitsu in 2005 [Fujitsu2005]. In 2007, Intel announced its 45-nm CMOS industrial process and revealed some key features about metal gates. The “Common Platform” [Common2007] including IBM, Chartered Semiconductor, Samsung and Infineon has set-up a 45-nm CMOS technology for commercial production in 2007. The transistor channels range from 25 nm to 40 nm in size (25 to 40 billionths of a meter). Some of the key features of the 45 nm technologies from various providers are given in Table 2.

Parameter	Value
V <sub>DD</sub> (V)	0.85-1.2 V
Effective gate length (nm)	25-40
Ion N ( $\mu\text{A}/\mu\text{m}$ ) at 1V	750-1000
Ion P ( $\mu\text{A}/\mu\text{m}$ ) at 1V	350-530
Ioff N (nA/ $\mu\text{m}$ )	5-100
Ioff P (nA/ $\mu\text{m}$ )	5-100
Gate dielectric	SiON, HfO <sub>2</sub>
Equivalent oxide thickness (nm)	1.1-1.5
# of metal layers	6-10
Interconnect layer permittivity K	2.2-2.6

Table 2: Key features of the 45 nm technology

Compared to 65-nm technology, most 45-nm technologies offer:

- 30 % increase in switching performance
- 30 % less power consumption
- 2 times higher density
- X 2 reduction of the leakage between source and drain and through the gate oxide

### Gate Material

For 40 years, the SiO<sub>2</sub> gate oxide combined with polysilicon have been serving as the key enabling materials for scaling MOS devices down to the 90nm technology node. One of the struggles the IC manufacturers went through was being able to scale the gate dielectric thickness to match continuous requirements for improved switching performance. But the leakage current between drain/source and the gate became significant.

The combination of high dielectric materials with polysilicon gate has revealed [Chau04, Intel] unexpected increase of

parasitic threshold voltage and severe degradation of the carrier mobility, which jeopardized the benefits of a scaled channel length. For the first time in 40 years of CMOS manufacturing, the poly gate has been abandoned. Nickel-Silicide (NiSi), Titanium-Nitride (TiN) etc. are the types of gate materials that provide acceptable threshold voltage and alleviate the mobility degradation problem (Fig. 3). It is interesting to note that most IC manufacturers do not reveal the exact structure of the metal gate. In combination with Hafnium Oxide ( $\text{HfO}_2$ ,  $\epsilon_r=12$ ), the metal/high-k transistors feature outstanding current switching capabilities together with low leakage. Increased *on* current, decreased *off* current and significantly decreased gate leakage are obtained with this novel combination.

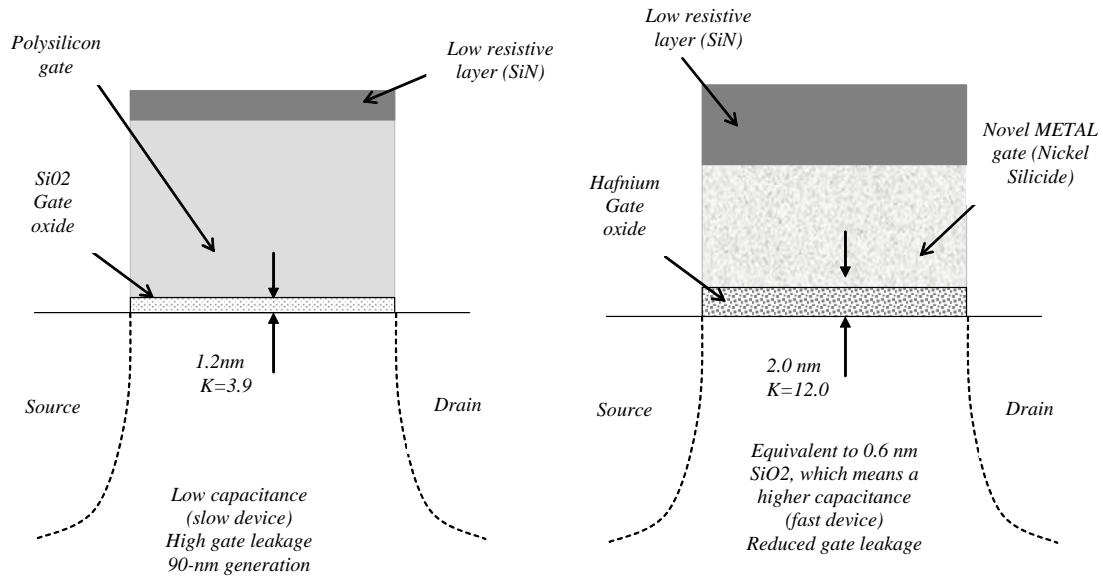


Figure 3: The metal gate combined with High-K oxide material enhance the MOS device performance in terms of switching speed and significantly reduce the leakage

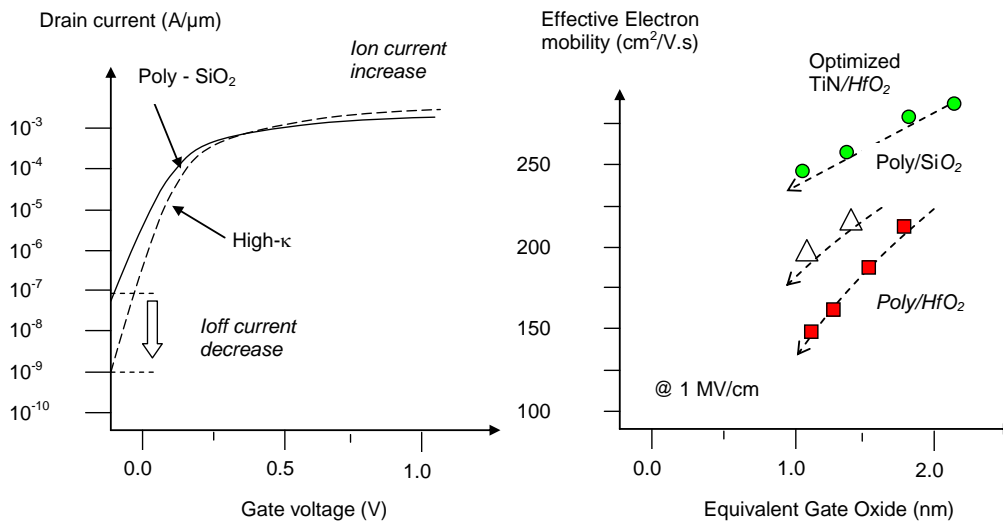


Figure 4: The metal gate combined with High-K oxide material enhances the Ion current and drastically reduces the Ioff current (left). Electron mobility vs. Equivalent gate oxide thickness for various materials (right).

The effective electron mobility is significantly reduced with a decrease of the equivalent gate oxide thickness, as seen in Fig. 4, which compiles information from [Chau2004] [Lee2005][Song2006]. It can be seen that the highest mobility is obtained with optimized TiN/HfO<sub>2</sub>, while Poly/ HfO<sub>2</sub> do not lead to suitable performances.

## Strained Silicon

Strained silicon has been introduced starting with the 90-nm technology [Sicard2005b], [Sicard2006b] to speed-up the carrier mobility, which boosts both the n-channel and p-channel transistor performances. PMOS transistor channel strain has been enhanced by increasing the Germanium (Ge) content in the compressive SiGe (silicium-germanium) film. Both transistors employ ultra shallow source-drains to further increase the drive currents.

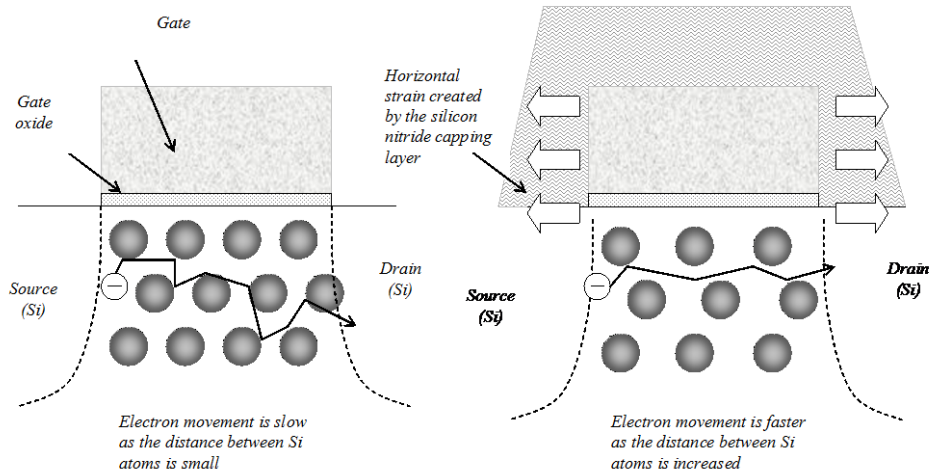


Figure 5: Tensile strain generated by a silicon-nitride capping layer which increases the distance between atoms underneath the gate, which speeds up the electron mobility of n-channel MOS devices

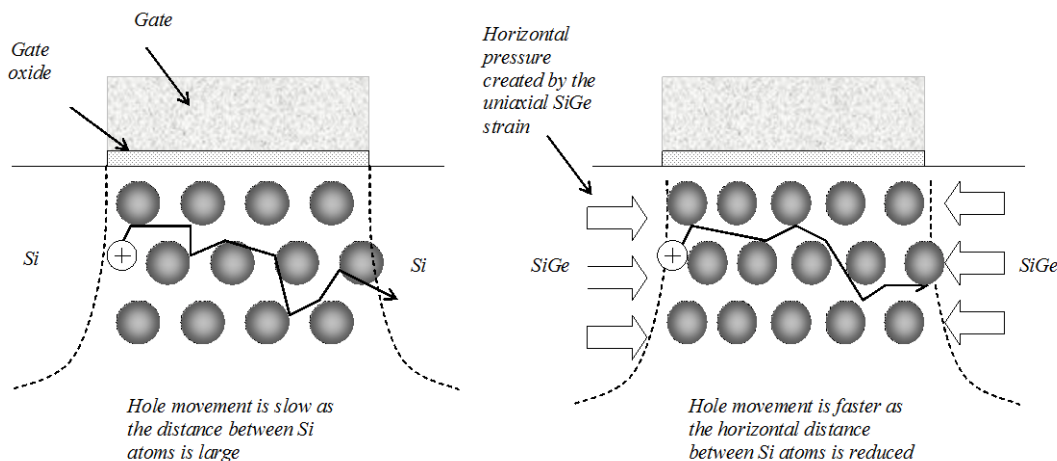


Figure 6: Compressive strain to reduce the distance between atoms underneath the gate, which speeds up the hole mobility of p-channel MOS devices

Let us assume that the silicon atoms form a regular lattice structure, inside which the carriers participating to the device current have to flow. In the case of electron carriers, stretching the lattice (by applying tensile strain) allows the electrons to flow faster from the source to the drain, as depicted in Fig. 5. The mobility improvement exhibits a linear dependence on the tensile film thickness. In a similar way, compressing the lattice slightly speeds up the p-type transistor, for which current carriers consist of holes (Fig. 6). The combination of reduced channel length, decreased oxide thickness and strained silicon achieves a substantial gain in drive current for both nMOS and pMOS devices.

### N-channel MOS device characteristics

The tool Microwind in its version 3.1 is configured by default in 45-nm technology. The default 45-nm technology uses a stack of high-k dielectric, metal (TiN) and polysilicon. Cross-sections of the n-channel MOS devices are given in Fig. 7. The nMOS gate is capped with a specific silicon nitride layer that induces lateral tensile channel strain for improved electron mobility.

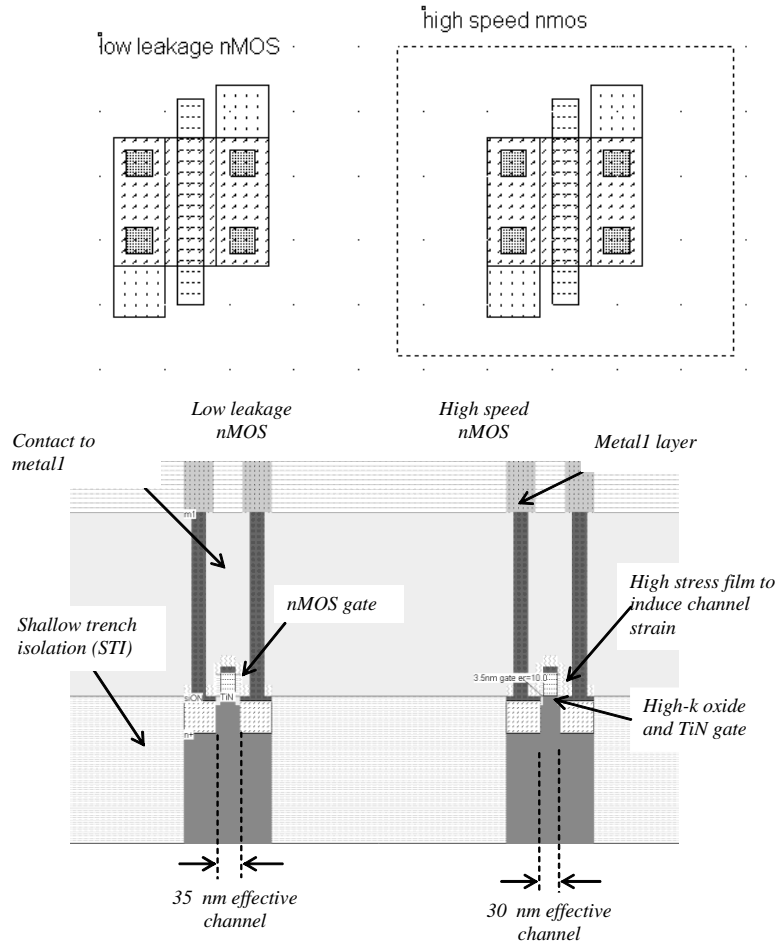
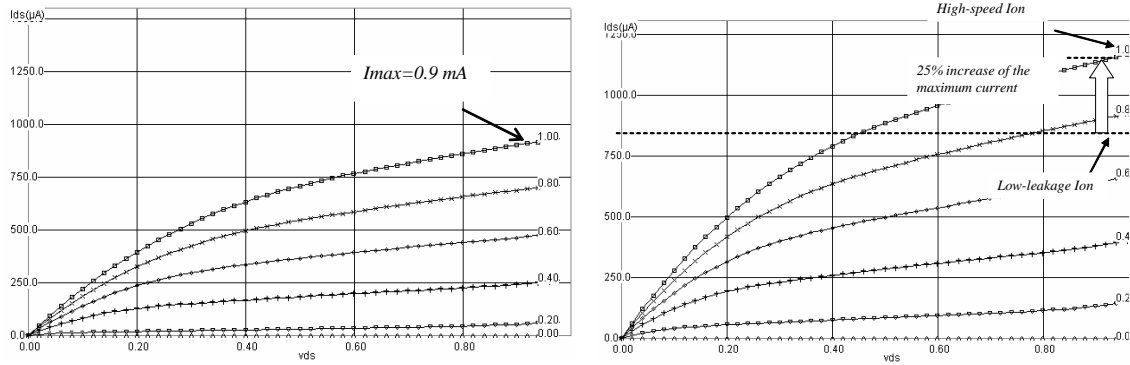


Figure 7: Cross-section of the nMOS devices (allMosDevices.MSK)

Parameter	NMOS Low leakage	NMOS High speed
Drawn length (nm)	40	40
Effective length (nm)	35	30
Threshold voltage (V)	0.20	0.18
Ion (mA/μm) at VDD=1.0V	0.9	1.2
Ioff (nA/μm)	7	200

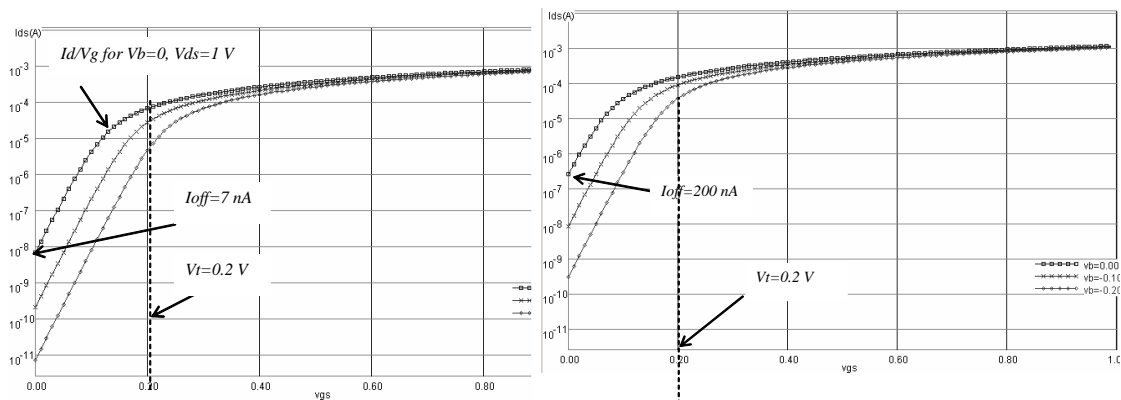
Table 3: nMOS parameters featured in the CMOS 45-nm technology provided in Microwind



(a) Low leakage  $W=1\mu\text{m}$ ,  $L_{\text{eff}}= 35\text{nm}$       (b) High speed  $W=1\mu\text{m}$ ,  $L_{\text{eff}}= 30\text{nm}$

Figure 8:  $I_d/V_d$  characteristics of the low leakage and high speed nMOS devices

The device I/V characteristics of the low-leakage and high-speed MOS devices listed in Table 3 are obtained using the MOS model BSIM4 (See [Sicard2005a] for more information about this model). The cross-section of the low-leakage and high-speed MOS devices do not reveal any major difference (Fig. 7), except a reduction of the effective channel length. Concerning the low-leakage MOS, the I/V characteristics reported in Fig. 8 demonstrate a drive current capability of around  $0.9 \text{ mA}/\mu\text{m}$  for  $W=1.0\mu\text{m}$  at a voltage supply of  $1.0 \text{ V}$ . For the high speed MOS, the effective channel length is slightly reduced as well as the threshold voltage, to achieve a drive current around  $1.2 \text{ mA}/\mu\text{m}$ .



(a) low leakage MOS ( $L_{\text{eff}}=35 \text{ nm}$ )      (b) high speed MOS ( $W=1 \mu\text{m}$ ,  $L_{\text{eff}}=30 \text{ nm}$ )

Figure 9:  $I_d/V_g$  characteristics (log scale) of the low leakage and high-speed nMOS devices

The drawback of the high-speed MOS current drive is the leakage current which rises from  $7 \text{ nA}/\mu\text{m}$  (low leakage) to  $200 \text{ nA}/\mu\text{m}$  (high speed), as seen in the  $I_d/V_g$  curve at the X axis location corresponding to  $V_g= 0 \text{ V}$  (Fig. 9-b).

### P-channel MOS device characteristics

The PMOS drive current in this 45-nm technology is around  $550 \mu\text{A}/\mu\text{m}$  for the low-leakage MOS and up to  $700 \mu\text{A}/\mu\text{m}$  for the high-speed MOS. These values (see Table 4) are not particularly high, as the target applications for this technology are low-power embedded electronics, in contrast with 45-nm technology targeted to ultra high-speed microprocessors (see Fig. 15 for an illustration of 45-nm technology variants). The leakage current is remarkably low, around  $5 \text{ nA}/\mu\text{m}$  for the low-leakage MOS and near  $180 \text{ nA}/\mu\text{m}$  for the high-speed device. The cross-section of the pMOS device reveals an SiGe material that induces compressive strain to obtain maximum current capabilities (Fig. 10).

Parameter	pMOS Low leakage	pMOS High speed
Drawn length (nm)	40	40
Effective length (nm)	35	30
Threshold Voltage (V)	0.19	0.17
Ion (mA/μm) at VDD=1.0V	0.55	0.70
Ioff (nA/μm)	5	180

Table 4: pMOS parameters featured by the 45-nm CMOS technology provided in Microwind

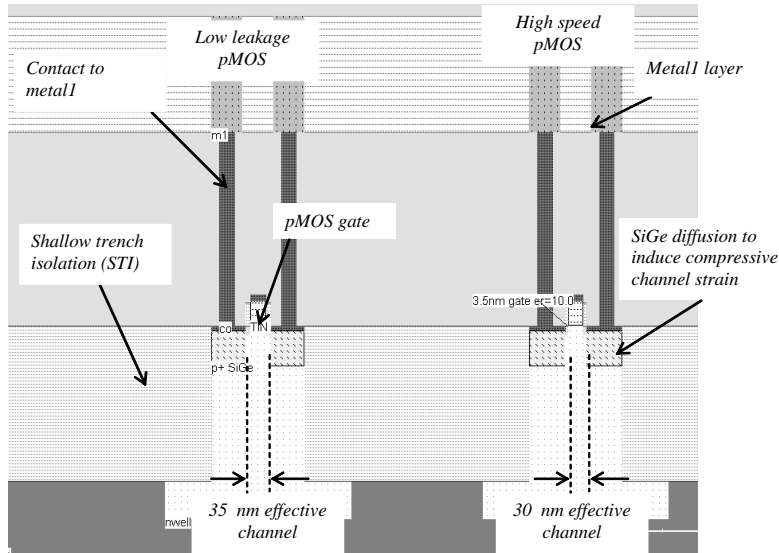


Figure 10: Cross-section of the pMOS devices

### Metal Layers

As seen in the palette (Fig. 11), the available metal layers in 45nm technology range from *metal1* to *metal8*. The layer *metal1* is situated at the lowest altitude, close to the active device, while *metal8* is nearly 10μm above the silicon surface. Metal layers are labeled according to the order in which they are fabricated, from the lower level (*metal1*) to the upper level (*metal8*).

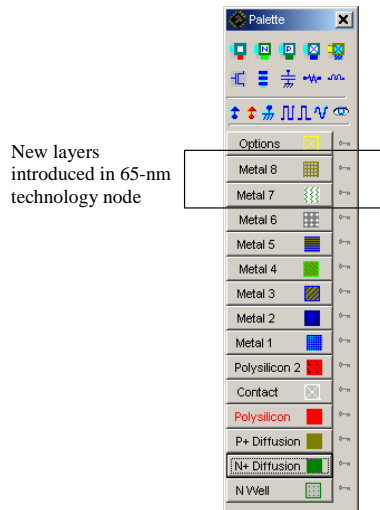


Figure 11: Microwind window with the palette of layers including 8 levels of metallization

In Microwind, specific macros are accessible to ease the addition of contacts in the layout. These macros can be found in the palette. As an example, you may instantiate a design-error free *metal7/metal8* contact by selecting *metal8*, followed by a click on the upper left corner icon in the palette. A *metal7/metal8* contact is depicted in Fig. 12. Additionally, access to complex stacked contacts is proposed thanks to the icon "complex contacts" situated in the

palette, in the second column of the second row. The screen shown in Fig. 13 appears when you click on this icon. By default it creates a contact from poly to *metal1*, and from *metal1* to *metal2*. Tick more boxes “between metals” to build more complex stacked contacts.

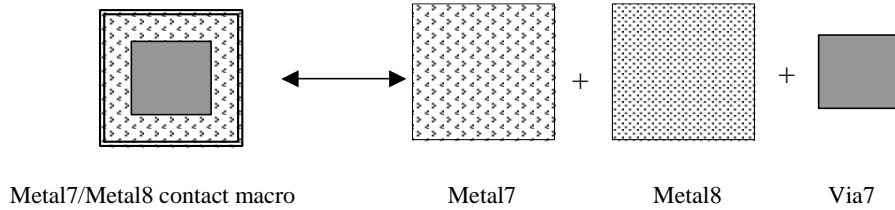


Figure 12: Access to contact macros between metal layers

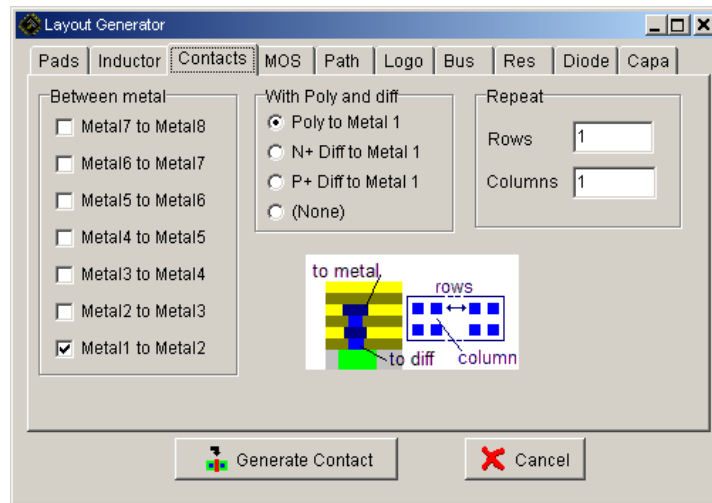


Figure 13: Access to complex contact generator

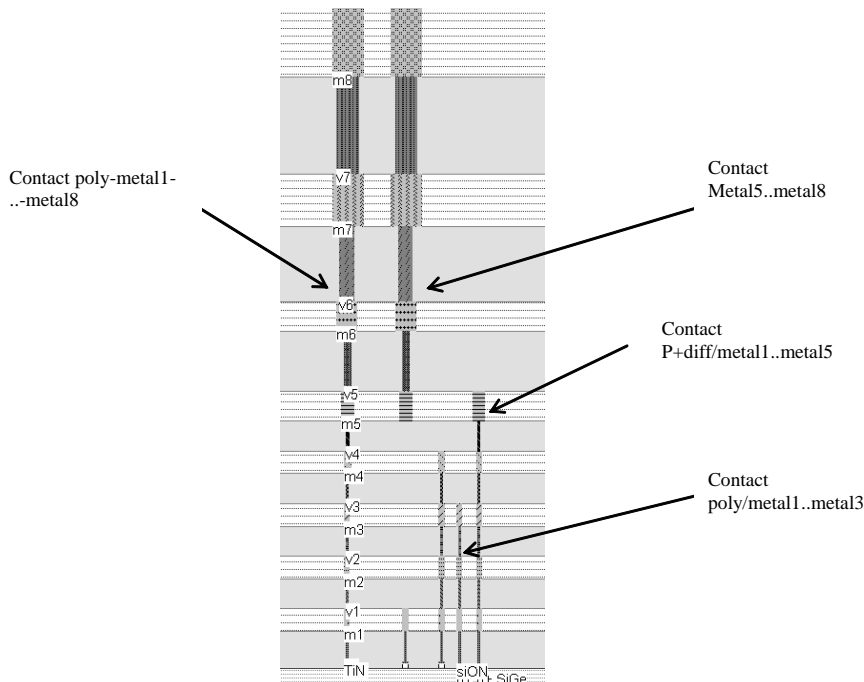


Figure 14: Examples of layer connection using the complex contact command from Microwind (Contacts.MSK)

Each layer is embedded into a low dielectric oxide (referred to as “interconnect layer permittivity K” in Table 2), which isolates the layers from each other. A cross-section of a 45-nm CMOS technology is shown in Fig. 14. In 45-nm technology, the layers *metal1..metal4* have almost identical characteristics. Concerning the design rules, the minimum

width  $w$  of the interconnect is  $3\lambda$ . The minimum spacing is  $4\lambda$ . Layers *metal5* and *metal6* are a little thicker and wider, while layers *metal7* and *metal8* are significantly thicker and wider, to drive high currents for power supplies. The design rules for *metal8* are  $25\lambda$  ( $0.5\mu\text{m}$ ) width,  $25\lambda$  ( $0.5\mu\text{m}$ ) spacing.

## 2. 45-nm process variants

There may exist several variants of the 45-nm process technology. One corresponds to the highest possible speed, at the price of a very high leakage current. This technology is called “High speed” as it is dedicated to applications for which the highest speed is the primary objective: fast microprocessors, fast DSP, etc. This technology has not been addressed in Microwind’s 45nm rule file.

The second technological option called “General Purpose” (Fig. 15) is targeted to standard products where the speed factor is not critical. The leakage current is one order of magnitude lower than for the high-speed variant, with gate switching decreased by 50%. Only this technology has been implemented in Microwind.

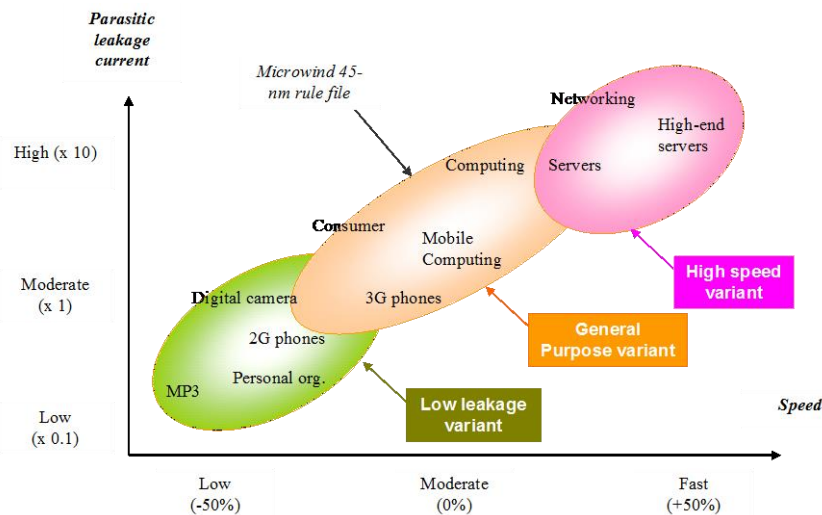


Figure 15 : Introducing three variants of the 45-nm technology

There may also exist a third variant called low leakage (bottom left of Fig. 15). This variant concerns integrated circuits for which the leakage current must remain as low as possible, a criterion that ranks first in applications such as embedded devices, mobile phones or personal organizers. The operational voltage is usually from 0.8 V to 1.2 V, depending on the technology variant. In Microwind, we decided to fix VDD at 1.0 V in the *cmos45nm.RUL* rule file, which represents a compromise between all possible technology variations available for this 45-nm node.

## MOS types

At least three types of MOS devices exist within the “General Purpose” variant of the 45-nm technology implemented in Microwind, which may be confusing as they partially reuse the technology terminology: the low-leakage MOS is the default MOS device, and the high-speed MOS has higher switching performance but higher leakage. The third MOS option is the high voltage MOS used for input/output interfacing. In Microwind’s *cmos45nm* rule file, the I/O supply is 1.8 V. Most foundries also propose 2.5 V and 3.3 V interfacing.

The main objective of the low leakage MOS is to reduce the  $I_{off}$  current significantly, that is the small current that

flows between drain and source with a zero gate voltage. The price to pay is a reduced  $I_{on}$  current. The designer has the choice of using high-speed MOS devices, which have high  $I_{off}$  leakages but large  $I_{on}$  drive currents.

### 3. Designing in 45 nm technology

#### Ring Inverter Simulation

The ring oscillator made from 5 inverters has the property of oscillating naturally. We observe the oscillating outputs in the circuit of Fig. 16 and measure their corresponding frequency.

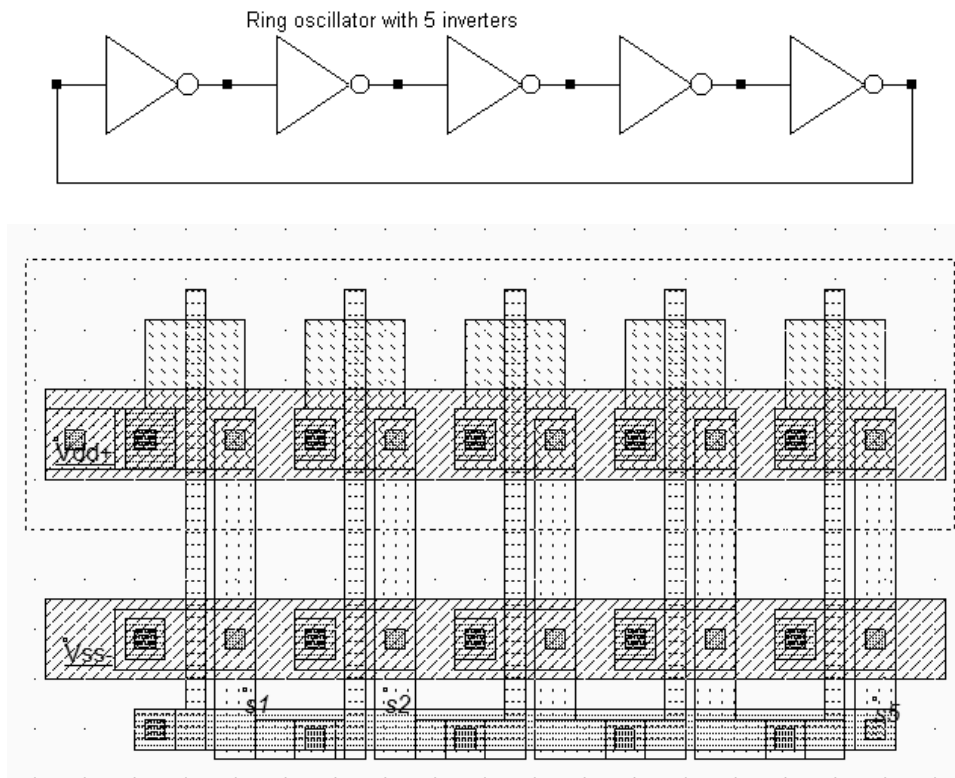


Figure 16: Schematic diagram and layout of the ring oscillator used for simulation (INV5.MSK)

The ring oscillator circuit can be simulated easily at layout level with Microwind using various technologies. The time-domain waveform of the output is reported in Fig. 17 for 0.8  $\mu\text{m}$ , 0.18  $\mu\text{m}$  and 45-nm technologies (high-speed option). Although the supply voltage (VDD) has been reduced (VDD is 5V in 0.8  $\mu\text{m}$ , 2V in 0.18 $\mu\text{m}$ , and 1.0 V in 45-nm), the gain in frequency improvement is significant.

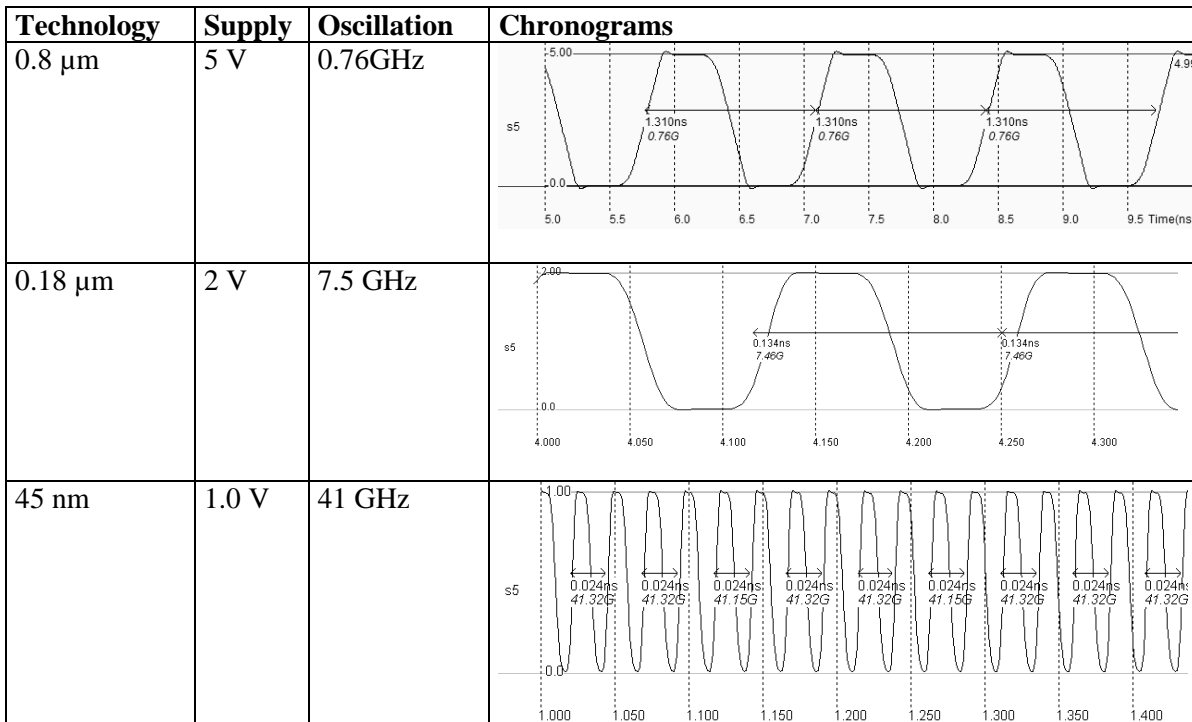


Figure 17: Oscillation frequency improvement with the technology scale down (Inv5.MSK)

Use the command **File** → **Select Foundry** to change the configuring technology. Select sequentially the **cmos08.RUL** rule file which corresponds to the CMOS 0.8- $\mu\text{m}$  technology, the **cmos018.RUL** rule file (0.18 $\mu\text{m}$  technology), and eventually **cmos45nm.RUL** which configures Microwind to the CMOS 45-nm technology. When you run the simulation, observe the change of VDD and the significant change in oscillating frequency.

### High Speed vs. Low leakage

Let us consider the ring oscillator with an enable circuit, where one inverter has been replaced by a NAND gate to enable or disable oscillation (Inv5Enable.MSK). The schematic diagram of the oscillator and its layout implementation are shown in Fig. 18. We analyze its switching performances, as shown in Fig. 19, in the high speed and low leakage modes.

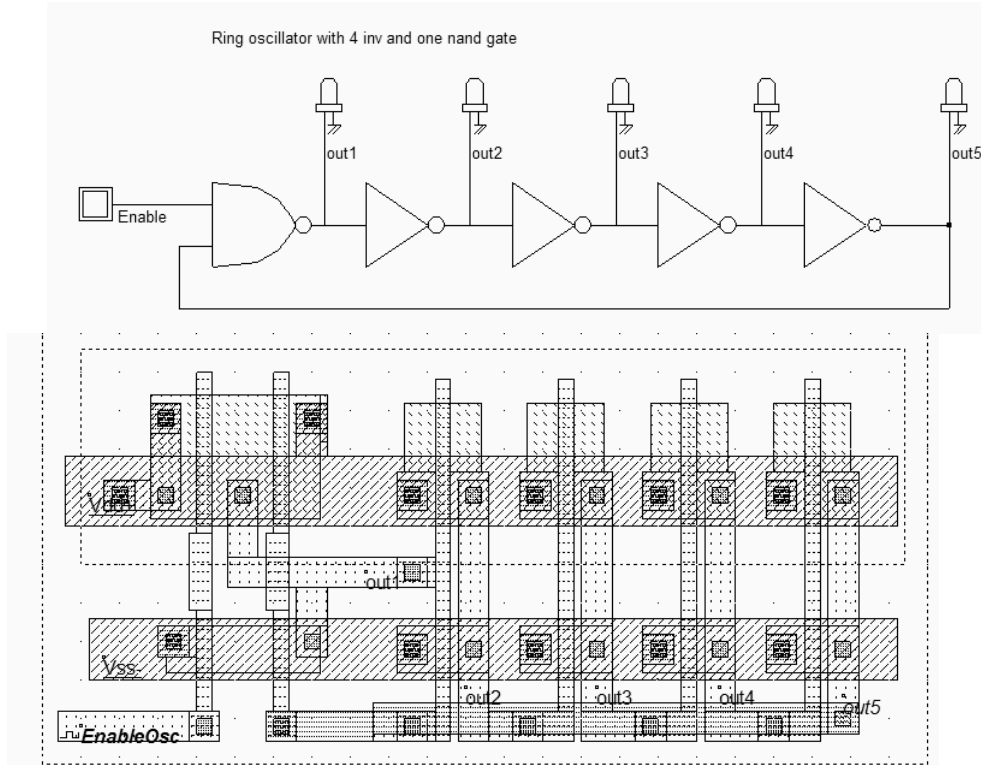


Figure 18 : The schematic diagram and layout of the ring oscillator used to compare the analog performances in high speed and low leakage mode (INV5Enable.MSK)

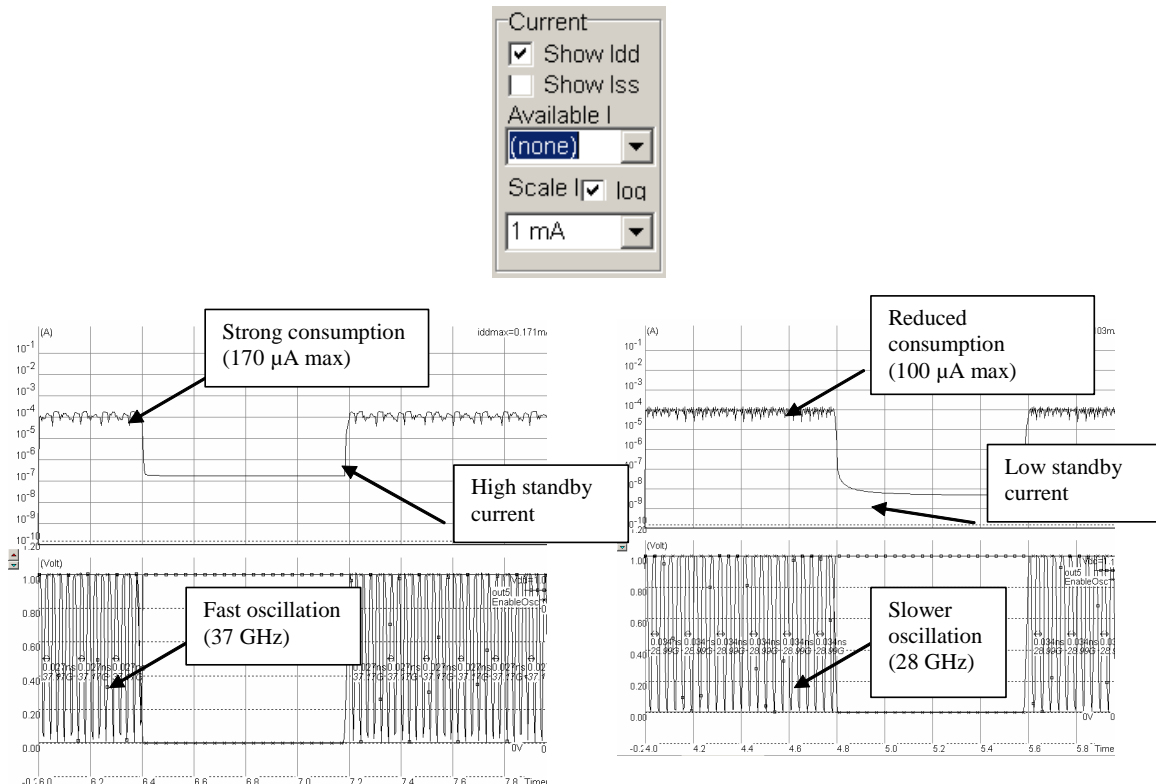


Figure 19: Simulation of the ring oscillator in high speed mode (left) and low leakage mode (right). The oscillating frequency is faster in the case of high-speed mode but the standby current is high (Inv5Enable.MSK)

The tick in front of "Scale I in log" must be asserted to display the current in logarithmic scale. The option layer which surrounds all the oscillator devices is set to high speed mode first by a double click inside that box, and by selecting "high speed" (Fig. 20). The analog performances of both options are summarized in Fig. 19. In the high speed mode, the circuit works fast (37 GHz) but consumes a significant standby current when off (around 200 nA).

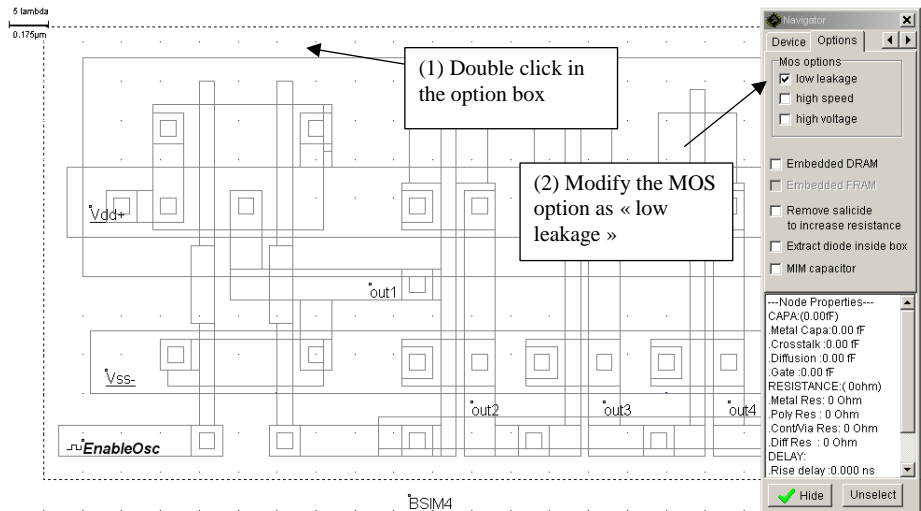


Figure 20: Changing the MOS option into low leakage mode

Once the option layer is set to “low leakage” (Fig. 20), the simulation is performed again. The low-leakage mode features a little slower oscillation (29 GHz that is approximately a 30 % speed reduction) and more than one decade less standby current when off (5 nA). In summary, low leakage MOS devices should be used as default devices whenever possible. High speed MOS should be used only when switching speed is critical.

### 6-transistor static RAM

One of the most representative design concerns the static RAM (6T-SRAM) cell designed using 6 transistors. Details about a real 45-nm 6T-SRAM can be found in [Fujitsu2005]. In our implementation in Microwind (see Figure 21), the layout size is 0.8 x 0.32  $\mu\text{m}$ , which is very close to published data (0.72 x 0.34  $\mu\text{m}$ ). Most contacts are shared with neighboring cells: the VSS, VDD contacts, the Select and Data lines. It is usual to find more aggressive layout design rules in RAM cell designs, in order to further decrease the cell area.

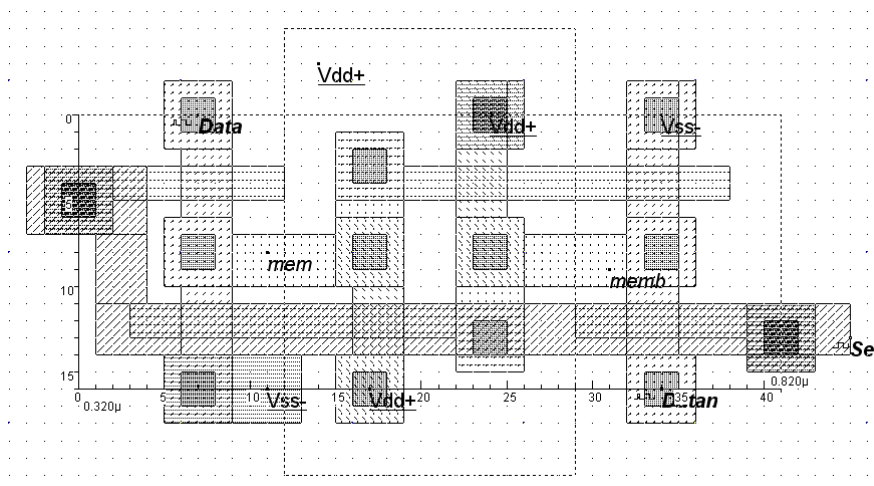


Figure 21: The 6-transistor RAM layout using 45-nm design rules (Ram6T\_45nm.MSK)

## 4. Conclusions

This application note has illustrated the trends in CMOS technology and introduced the 45-nm technology generation, based on technology information available from integrate circuit manufacturers. A set of specific topics has been addressed, including the new gate dielectric, gate stack and the strained silicon technique for enhanced mobility, the 8-metal interconnect back-end process and the 45-nm process variants. N-channel and P-channel MOS device characteristics have been presented, as well as a comparative study of a ring inverter oscillator for various technology nodes. Finally, performances of the ring oscillator in the high speed and low leakage modes have been compared, with the impact on speed and leakage current. Future work will concern the 32-nm technology node, under preparation for an industrial production in 2010, which could include double-gate MOS devices.

## References

- [Chau2004] R. Chau « Gate Dielectric Scaling for High-Performance CMOS : From SiO<sub>2</sub> to High-K », IEDM Technical Digest, 2004
- [Common2007] The Common Platform technology model is focused on 90-nm, 65-nm and 45-nm technology <http://www.commonplatform.com/home>
- [Fujitsu2005] Okuno M. and al. « 45-nm Node CMOS Integration with a Novel STI Structure and Full-NCS/Cu Interlayers for Low-Operation-Power (LOP) Applications », Fujitsu Laboratories Ltd, proceedings of IEDM 2005
- [Lee2005] Lee, B.H, “Challenges in implementing high-k dielectrics in the 45nm technology node.”, 2005 International Conference on Integrated Circuit Design and Technology, ICICDT, May 2005 pp. 73 – 76
- [Nec2007] M. Tada “Feasibility Study of 45-nm-Node Scaled-Down Cu Interconnects With Molecular-Pore-Stacking (MPS) SiOCH Films, IEEE Trans. On Electron Devices, Vol. 54, No. 4, April 2007
- [Osishi2005] Oishi, A “High performance CMOSFET technology for 45nm generation and scalability of stress-induced mobility enhancement technique”, IEEE International Electron Devices Meeting, 2005. IEDM Technical Digest. 2005 pp. 229 - 232
- [Song2006] S.C. Song “Highly Manufacturable Advanced Gate-Stack Technology for Sub 45-nm Self Aligned Gate-First CMOSFETs”, IEEE Trans. On Electron Devices, Vol. 53, pp 979-989, May 2006
- [Sicard2005a] E. Sicard, S. Ben Dhia “Basic CMOS cell design”, McGraw Hill India, 450 pages, ISBN 0-07-0599335, June 2005 (international edition to appear 2007)
- [Sicard2005b] E. Sicard “Introducing 90-nm technology in Microwind3”, application note, July 2005, [www.microwind.org](http://www.microwind.org)
- [Sicard2006a] E. Sicard “Microwind User’s Manual, lite version 3.1”, [www.microwind.org](http://www.microwind.org), INSA editor, 2006
- [Sicard2006b] E. Sicard “Introducing 65-nm technology in Microwind3”, application note, July 2006, [www.microwind.org](http://www.microwind.org)
- [Tsmc2004] Yang F. L and al. “45nm node planar-SOI technology with 0.296μm<sup>2</sup> 6T-SRAM cell”, Digest of Technical Papers, Symposium on VLSI Technology, 15-17 June 2004 pp 8-9.
- [Tsai2003] W. Tsai, “Performance Comparison of Sub 1 nm Sputtered TiN/HfO<sub>2</sub> nMOS and pMOSFETs,” IEDM Tech. Digest, p. 311 (2003).